AD-A067 336 AEROSPACE CORP EL SEGUNDO CALIF AEROPHYSICS LAB F/G 9/5
IMPROVED CAMERA-TUBE PERFORMANCE WITH PULSED OPERATION.(U)
FEB 79 E F CROSS, J M NARDUZZI F04701-78-C-0079
UNCLASSIFIED TR-0079(4920)-1 SAMSO-TR-79-21 NL

END
DATE FILMED
6-79
DDC

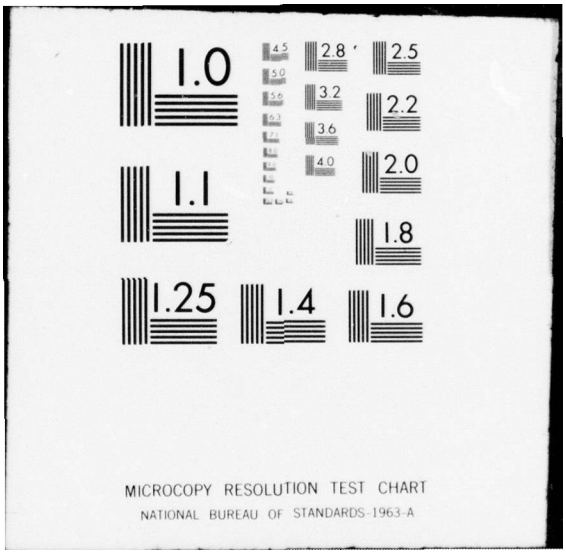
1.0
1.1
1.25
1.4
1.6
1.8
2.0
2.2
2.5
2.8
3.2
3.6
4.0
4.5
5.0
5.6
MICROCOPY RESOLUTION TEST CHART
NATIONAL BUREAU OF STANDARDS-1963-A

REPORT SAMSO-TR-79-21

LEVEL II 12

AD A067336

DDC FILE COPY

Improved Camera-Tube Performance with Pulsed Operation

E. F. CROSS and J. M. NARDUZZI
Aerophysics Laboratory
Laboratory Operations
The Aerospace Corporation
El Segundo, Calif. 90245

DDC RECEIVED APR 16 1979 C

27 February 1979

Interim Report

APPROVED FOR PUBLIC RELEASE;
DISTRIBUTION UNLIMITED

Prepared for

SPACE AND MISSILE SYSTEMS ORGANIZATION
AIR FORCE SYSTEMS COMMAND
Los Angeles Air Force Station
P.O. Box 92960, Worldway Postal Center
Los Angeles, Calif. 90009

79 04 10 012

This interim report was submitted by The Aerospace Corporation, El Segundo, CA 90245, under Contract No. F04701-78-C-0079 with the Space and Missile Systems Organization, Contracts Management Office, P.O. Box 92960, Worldway Postal Center, Los Angeles, CA 90009. It was reviewed and approved for The Aerospace Corporation by W. R. Warren, Director, Aerophysics Laboratory. Gerhard E. Aichinger was the project officer for Mission-Oriented Investigation and Experimentation (MOIE) Programs.

This report has been reviewed by the Information Office (OI) and is releasable to the National Technical Information Service (NTIS). At NTIS, it will be available to the general public, including foreign nations.

This technical report has been reviewed and is approved for publication. Publication of this report does not constitute Air Force approval of the report's findings or conclusions. It is published only for the exchange and stimulation of ideas.

Gerhard E. Aichinger
Project Officer

FOR THE COMMANDER

Frank J. Bane, Chief
Contracts Management Office

UNCLASSIFIED

SECURITY CLASSIFICATION OF THIS PAGE *(When Data Entered)*

REPORT DOCUMENTATION PAGE	READ INSTRUCTIONS BEFORE COMPLETING FORM
1. REPORT NUMBER: SAMSO-TR-79-21	2. GOVT ACCESSION NO.
3. RECIPIENT'S CATALOG NUMBER	
4. TITLE *(and Subtitle)*: IMPROVED CAMERA-TUBE PERFORMANCE WITH PULSED OPERATION	5. TYPE OF REPORT & PERIOD COVERED: Interim rept.
6. PERFORMING ORG. REPORT NUMBER: TR-0079(4920)-1	
7. AUTHOR(s): Edward F. Cross and Joseph M. Narduzzi	8. CONTRACT OR GRANT NUMBER(s): F04701-78-C-0079
9. PERFORMING ORGANIZATION NAME AND ADDRESS: The Aerospace Corporation, El Segundo, Calif. 90245	10. PROGRAM ELEMENT, PROJECT, TASK AREA & WORK UNIT NUMBERS
11. CONTROLLING OFFICE NAME AND ADDRESS: Space and Missile Systems Organization, Air Force Systems Command, Los Angeles, Calif. 90009	12. REPORT DATE: 27 February 1979 13. NUMBER OF PAGES: 29
14. MONITORING AGENCY NAME & ADDRESS *(if different from Controlling Office)*: 33p.	15. SECURITY CLASS. *(of this report)*: Unclassified 15a. DECLASSIFICATION/DOWNGRADING SCHEDULE

16. DISTRIBUTION STATEMENT *(of this Report)*

Approved for public release; distribution unlimited

17. DISTRIBUTION STATEMENT *(of the abstract entered in Block 20, if different from Report)*

18. SUPPLEMENTARY NOTES

19. KEY WORDS *(Continue on reverse side if necessary and identify by block number)*

Camera-Tube Performance
Image Device
Image Enhancement
Image-Tube Performance
Video-Frame Enhancement
Video-Signal Integration
Vidicon Sensitivity

20. ABSTRACT *(Continue on reverse side if necessary and identify by block number)*

A new electronic technique is discussed for improving the performance of a wide range of camera tubes (vidicons). Specifically, this technique significantly increases vidicon sensitivity by synchronously controlling the sensing-layer bias. Operational principles governing this new technique are explained in terms of the standard physical model that describes vidicon performance. The two pulsed operation methods discussed in this paper are referred to as the integrated-saturation and discharge modes. → next page

DD FORM (FACSIMILE) 1473

UNCLASSIFIED

SECURITY CLASSIFICATION OF THIS PAGE *(When Data Entered)*

79 04 10 012
409367 LB

19. KEY WORDS (Continued)

20. ABSTRACT (Continued)

The video-signal enhancement is achieved in real time without requiring any computer-signal processing or additional data-reduction circuitry. Two other noteworthy features of this electronic technique are that image enhancement can be achieved without detrimentally affecting other tube parameters and be monitored with standard television equipment.

The video enhancement anticipated with this synchronous pulse technique was verified experimentally. Four types of different camera tubes were tested in both the integrated-saturation and discharge pulsed modes. Specifically, standard visible light, silicon diode, photoconductive-infrared, and thermistor-infrared vidicons were used for the laboratory evaluation. These experimental results are presented in detail, together with quantitative comparisions of how each vidicon performed under conventional operation sensitivity. The measured improvement factor in threshold sensitivity ranged from approximately 3.0 to 6.0, depending on vidicon and pulsed mode. The results also indicated that dynamic range, in most cases, increased by approximately 50% while other vidicon transfer characteristics remained unaffected by pulsed mode operations.

CONTENTS

FIGURES

TABLE

PRECEDING PAGE NOT FILMED
BLANK

I. INTRODUCTION

Improving image-sensing parameters is a high-priority goal in the development of camera-tube (vidicon) television systems. In past efforts to enhance video output from these television systems the emphasis has been on multiple-frame integrations of a single scene and computer data processing of the recorded video. In the electronic technique discussed in this paper vidicon performance is improved by synchronously controlling the sensing-layer bias. Specifically, camera-tube sensitivity and dynamic response are significantly increased while other tube parameters remain unaffected. The resultant enhanced video, whether live or recorded, can be measured on a line-selector oscilloscope or qualitatively observed on a television monitor.

PRECEDING PAGE NOT FILMED
BLANK

II. PHYSICAL MODEL OF VIDICON OPERATION

This new video-enhancement technique can be analyzed in terms of the established physical model for vidicon operation. A standard vidicon consists of a light-sensitive retina assembly and a electronically controlled readout beam. The retina assembly consists of a window material on which is deposited a transparent thin-film electrode and a highly resistive photoconductive sensing layer (Fig. 1). In normal operation an optical system focuses scene imagery onto the front surface of the photoconductive sensing layer while the back surface is scanned with a magnetically or electrostatically focused electron beam. The film electrode electrically connects a constant positive bias voltage to the front photoconductive surface of the sensing layer as the back surface is stabilized sequentially to the cathode potential by the electron beam on an element-by-element basis. Incoming irradiance is only slightly decreased by the window and electrode film in the optical path because these retinae components are designed to have high transmission efficiencies in the spectral region of the photoconductor.

Each vidicon sensing-layer element can be described electronically as a small capacitor c_e of constant value shunted by a variable resistance r_e. The value for r_e varies inversely with the intensity of the incoming irradiance H_{sl} and the magnitude of the applied bias voltage V_{sl} (Fig. 2a).

During normal vidicon operation each c_e is fully charged to V_{sl} in sequence by a scanning beam used as a switch. Then during the elapsed time between two successive beam scans of the same sensing-layer element the charge on the c_e partially discharges through the r_e, causing the potential on the outside surface of the sensing layer to rise toward V_{sl}. This voltage discharge cycle for signal and no-signal conditions is shown as a function of time in Fig. 2b. The time interval between beam scans is the frame time T_F. Usually V_{sl} is set a value such that when there is no

PRECEDING PAGE NOT FILMED
BLANK

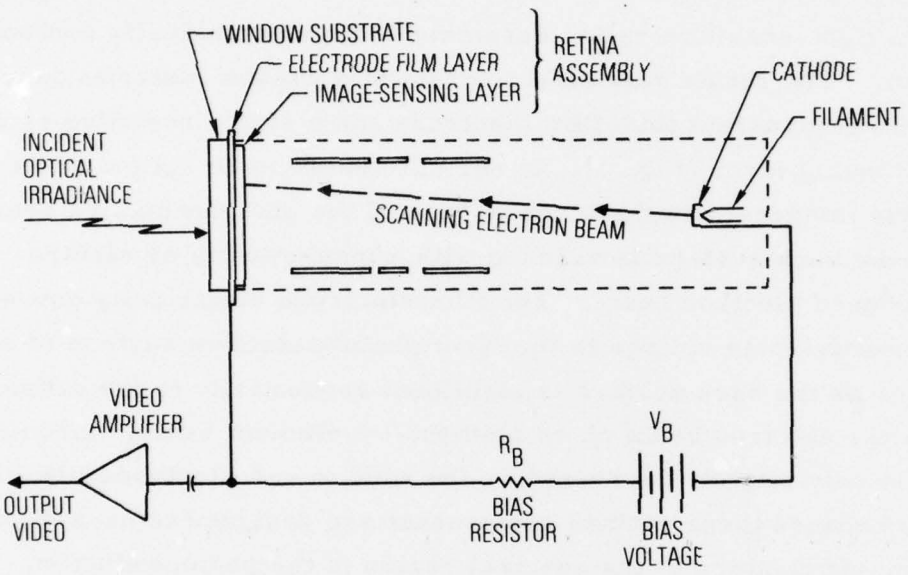

Fig. 1. Camera-Tube Operation

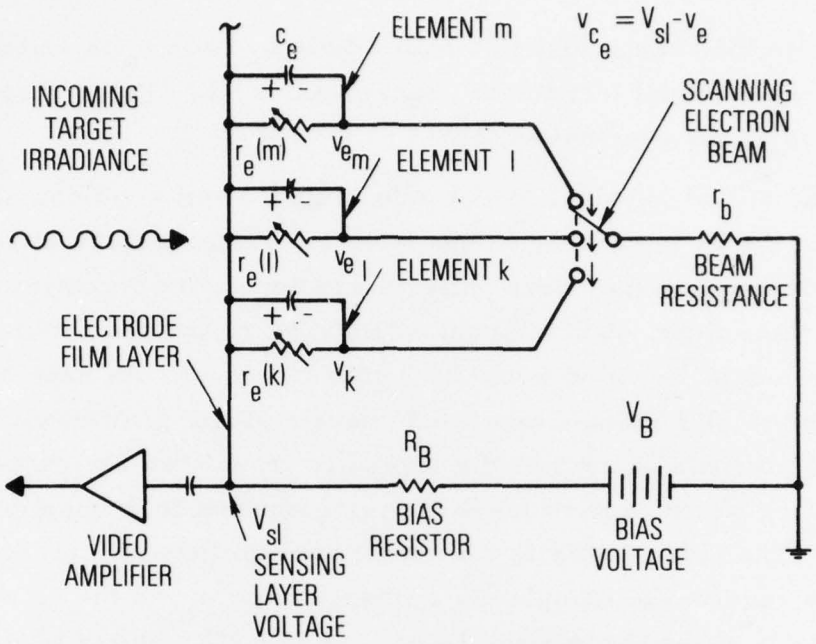

a. EQUIVALENT CIRCUIT FOR CAMERA-TUBE OPERATION

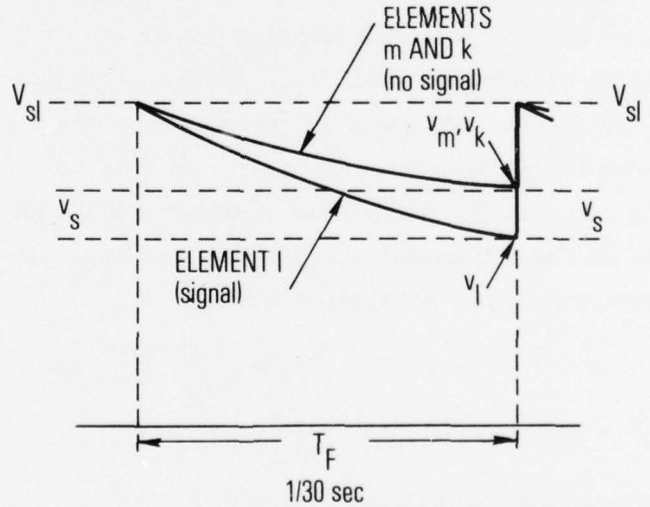

b. INSTANTANEOUS VOLTAGES ACROSS c_e's DURING CAMERA-TUBE OPERATION

Fig. 2. Physical Model of Camera-Tube Operation

signal irradiance the charge lost in a frame time by each c_e is relatively small but that when signal irradiance reaches any r_e the charge loss in c_e on that element increases proportionately.

By means of this physical model video output from a vidicon also can be described in terms of current pulses from individual picture elements. If all sensing-layer elements were uniform and none were irradiated during the previous frame time, each element would require the same charging current, and the derived video would be a constant level. As seen on a television monitor this video frame would have a single gray level. If however some portions of the sensing layer are irradiated the corresponding elements then would require more charging current in proportion to the radiant level. The video output is the result of amplitude differences in the current pulses required to completely recharge each c_e as the electron beam sequentially scans the sensing layer. On the TV monitor these pulse amplitudes correspond to a video pattern of multiple gray levels. As previously discussed the r_e for each sensing-layer element not only decreases with irradiation level but also with V_{sl}. In fact V_{sl} can be increased to a point where r_e is so low that each c_e loses more charge in one frame time than can be restored by the scanning beam. In this operational mode the amplitude of the current pulses will be equal to the video output, which is uniformly white on the TV monitor. The bias voltage at which this effect occurs is the sensing-layer saturation voltage V_{sls}.

III. THEORY OF OPERATION FOR IMPROVED-PERFORMANCE TECHNIQUE

The two methods for improving camera-tube performance by synchronously pulsing the sensing layer are the integrated-saturation and integrated-discharge modes. Both operational modes significantly increase camera-tube sensitivity and dynamic response. Determining which technique to use for optimum signal enhancement is dependent upon the type of vidicon selected.

In the integrating-saturation mode sensing-layer bias is switched from the standard steady-state value $V_{sl}(L)$ to a higher level $V_{sl}(H)$ for several frame times T_F, with video signal readout occurring when the sensing-layer bias returns to $V_{sl}(L)$. Under these operating conditions signal enhancement is produced during the saturation phase when the sensing layer-bias is at $V_{sl}(H)$. Saturation occurs when individual sensing-layer elements lose more charge in one frame time than the scanning beam can supply during recharge. This saturation effect is identical to that observed in standard vidicon cameras when V_{sl} is raised above normal recommended values. It is seen on the television monitor as a picture losing contrast, and becoming uniformly white.

Figure 3 is a diagram of typical voltage-time waveforms across adjacent c_e's for the integrated-saturation mode as V_{sl} is synchronously pulsed. In this specific analysis the selected pulse widths for $V_{sl}(L)$ and $V_{sl}(H)$ are one and two frame times, respectively. However, some additional sensitivity can usually be obtained by increasing the number of frame times at $V_{sl}(H)$ to three or more. The c_e's for both elements shown in this figure are completely charged by the scanning beam to the normal sensing-layer voltage $V_{sl}(L)$. After the beam leaves each element the voltage across the c_e begins to discharge exponentially toward zero. Because one element is being irradiated and the adjacent element is not

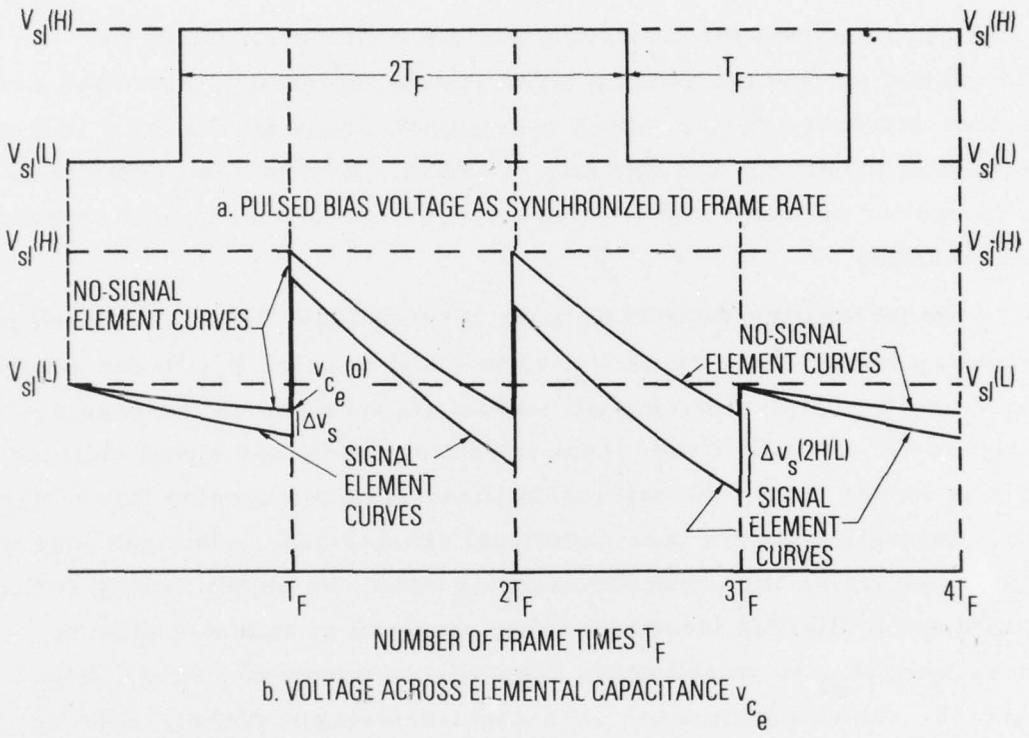

Fig. 3. Voltage-Time Waveforms for Pulsed Operation in Integrated-Saturation Mode

the discharge rates are different, which result in a different charge on the two elements at the end of one frame time T_F. When the beam returns at the end of one frame time to recharge the elements, the sensing-layer voltage is switched to a higher value above saturation $V_{sl}(H)$. At this $V_{sl}(H)$ the beam can fully recharge the no-signal element but cannot fully recharge the signal element. The charge-loss differential is proportional to the magnitude of the incoming signal irradiance and is retained (or stored) as the initial starting level for the elemental discharge during the first $V_{sl}(H)$ frame. This initial condition combined with the lower r_e produced by the signal irradiance and $V_{sl}(H)$ level significantly increases the charge differential between signal and no-signal elements at the end of the first $V_{sl}(H)$ frame. During the second $V_{sl}(H)$ frame this process is repeated with the initial starting point reflecting the greater charge differential obtained at the end of the first $V_{sl}(H)$ frame. Under these conditions the magnitude of charge loss by each signal element is approximately doubled during the second $V_{sl}(H)$ frame time. The total charge differential accumulated during the previous $V_{sl}(L)$ frame and both $V_{sl}(H)$ frames on each signal element is read out by the scanning electron beam when the sensing-layer bias is switched back to $V_{sl}(L)$. With the sensing-layer bias returned to the original $V_{sl}(L)$ value the beam again can fully charge each element, and the enhancement technique can be reinitiated from this point. By periodically repeating this electronic process increased video signals are produced on every third video frame when sensing-layer bias is at $V_{sl}(L)$.

In the integrated-discharge mode the sensing layer is switched from the normal $V_{sl}(L)$ level to a lower level $V_{sl}(0)$ at or near zero volt for two or more frame times. The image enhancement produced with this technique is achieved by integrating the charge loss across each c_e, which corresponds to the radiant intensity level. During the $V_{sl}(0)$ frame times the election beam is prevented from recharging individual the c_e's to $V_{sl}(L)$, and v_{c_e} decreases exponentially. When the sensing-layer bias

returns to $V_{sl}(L)$ differential v_{c_e}'s, i.e., $v_{c_e}(0) - v_{c_e}(s)$, which result from $V_{sl}(0)$ frame integration, constitute the enhanced video output. Figure 4 is a diagram of typical voltage-time waveforms across adjacent c_e's for the integrated-discharge mode as the sensing-layer bias is synchronously pulsed. A $V_{sl}(H)/V_{sl}(L)$ pulse ratio of one-third was selected for this analysis, but the ratio can be varied to accommodate the type of camera-tube and television-system considerations. The c_e for both sensing-layer elements shown in Fig. 4 are charged to $V_{sl}(L)$ by the scanning beam. After the beam leaves each element, the c_e begins to discharge at a rate determined by the r_e value for each element. When the beam returns to these adjacent elements during the next three frame times, neither c_e is recharged because V_{sl} has been switched to a value near zero $V_{sl}(0)$. The amount of discharge at $V_{sl}(L)$ consequently is carried over and added to the discharges that occur during the $V_{sl}(0)$ frames. The resultant integrated-charge differential between the signal and no-signal elements is then read out when V_{sl} returns to $V_{sl}(L)$. This technique is equivalent to cutting off the scanning election beam for several frame times and reading out the integrated video frame produced when the beam is switched back on.

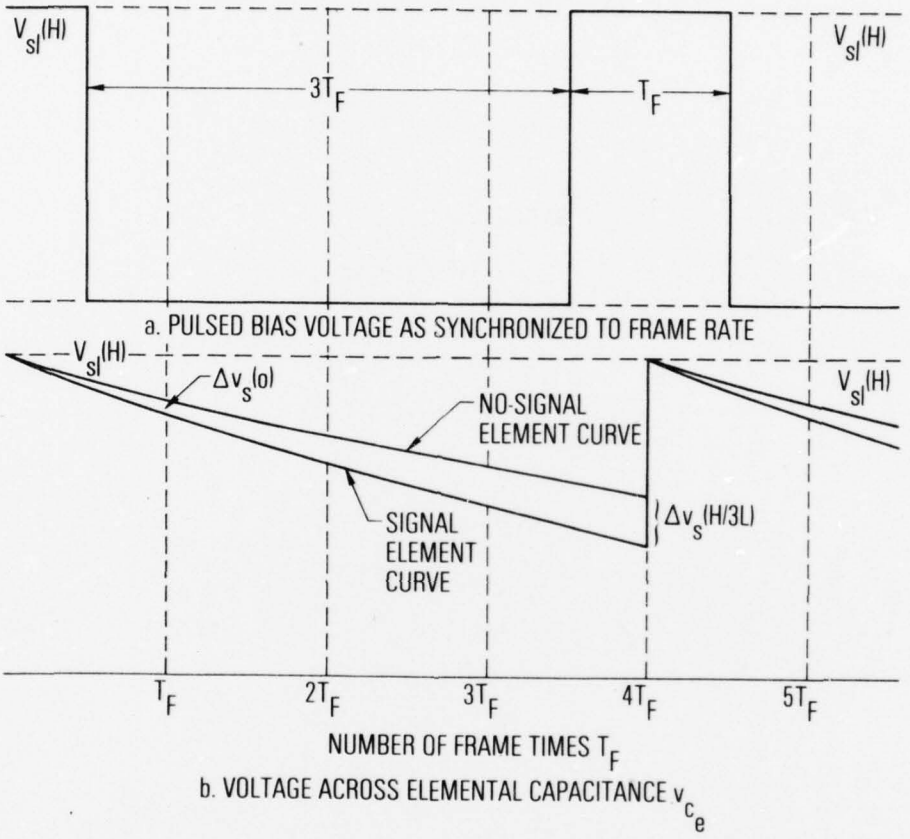

Fig. 4. Voltage-Time Waveforms for Pulsed Operation in Integrated-Discharge Mode

IV. EXPERIMENTAL TECHNIQUE

Five different camera tubes were used to experimentally verify the improved performance predicted by synchronously pulsing the sensing-layer bias. The three infrared sensitive vidicons tested have all-electrostatic guns with dynode structures for return-beam multiplication of video signals. With this electro-optical configuration video modulation on the return beam reaching the dynodes is electrically isolated from the pulsating-bias voltage on the tube sensing layer. Both visible-light-sensitive vidicons tested have standard electromagnetic gun structures with video output taken directly off the sensing layer. For this camera tube design the buffer circuit was inserted at the tube output to clamp the direct current component of the video at a constant level not affected by the pulsating-bias voltage (Fig. 5).

The increased video enhancement attained with this new technique was measured in terms of vidicon transfer characteristics as specified by the IRIS Standards for Infrared Camera Tubes (Refs. 1 and 2). These transfer characteristics curves describe video signal-to-envelope noise ratio (V_s/V_{en} dimensionless) as a function of signal irradiance reaching the camera-tube faceplate H_s in watts per square centimeter. In accordance with these aforementioned standards the numerical criteria used to specify vidicon sensitivity is envelope noise equivalent irradiance (NEH). This derived quantity, NEH, is defined as an H_s value that produces an output V_s/V_{en} equal to one. Also derived from the transfer characteristics curve is the dynamic response DR, which is the ratio of maximum signal irradiance short of saturation $H_{s(sat)}$ to the NEH. DR can also be defined as the range

---

[1] "Proposed Standards for Measurements on Infrared Camera Tubes Report of the Working Panel," Specialty Group on Infrared Image-Forming Sensors, Proceedings of IRIS 8 51-59 (1963).

[2] "Determination of Infrared Camera Tube Characteristics Report of the Working Panel," Specialty Group on Infrared Image-Forming Sensors, Proceedings of IRIS 10 49-55 (1966).

PRECEDING PAGE NOT FILMED BLANK

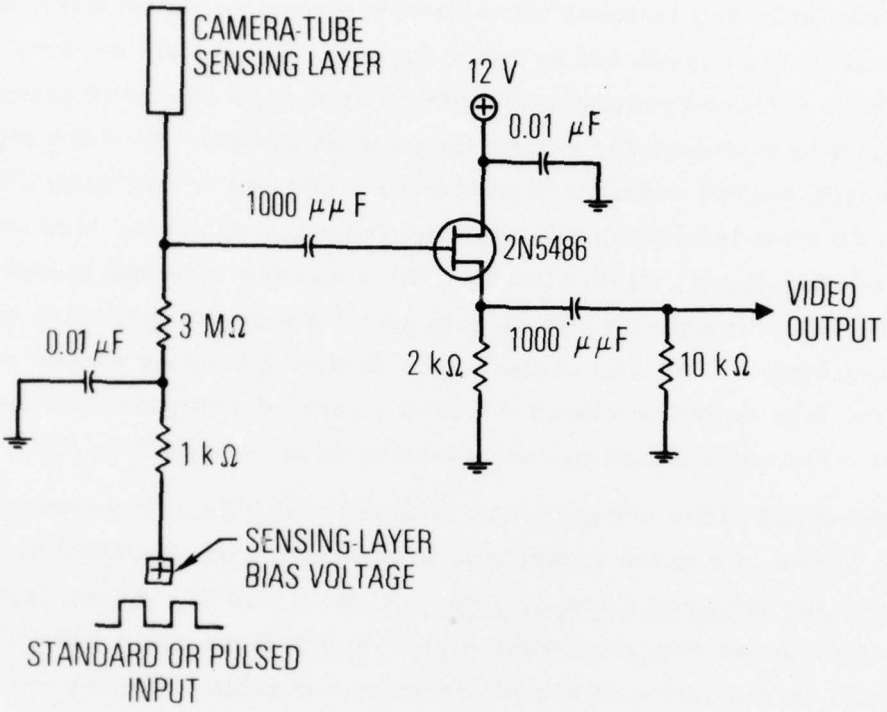

Fig. 5. Circuit Diagram for Isolating Video Output During Pulsed Operation

over which the slope of the transfer curve V_s/V_{en} versus H_s remains essentially constant.

In these laboratory measurements each vidicon tested was set up with the required optics and video electronics to view a standard blackbody source. For each test a spectral filter was placed in the optical path to limit all incoming irradiance to a wavelength region within the spectral response of the camera tube. Thus significant improvements in sensitivity would not become background limited, and wavelength region could be reliably specified for accurate measurement of tube transfer characteristics.

The blackbody source used has a 1.27-cm-diameter aperture and produces stable temperature levels in the 700 to 800°C range. Target irradiance levels for the infrared vidicons were varied by fixed amounts by placing neutral-density filters in front of the blackbody aperture. The V_s/V_{en} corresponding to the selected irradiance levels of the target was measured on a line-selector oscilloscope for each selected irradiance level. Typical oscilloscope presentations of V_s/V_{en} for a single-picture line, together with the television monitor displays during standard and pulsed operations, are shown in Fig. 6. Since the blackbody and optical parameters were known the signal irradiance at the sensing layer H_s could then be calculated for each V_s/V_{en} value.

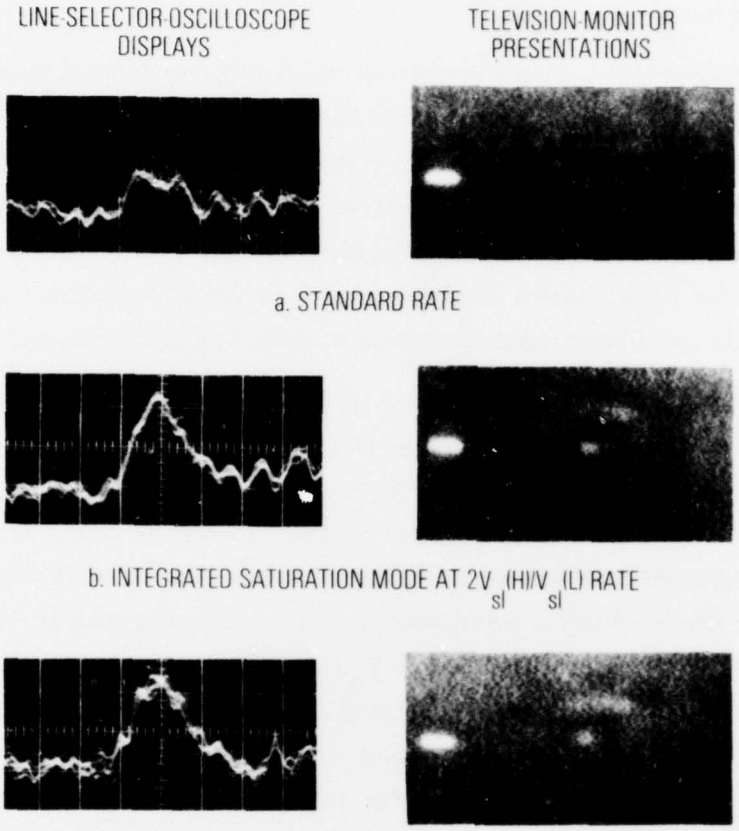

Fig. 6. Typical Video Signals for Standard Visible-Light Vidicon at Standard and Pulsed Operations

V. TEST RESULTS

The RCA Iricons used to evaluate this technique have an intrinsic photoconductive sensing layer of deposited lead telluride cooled to liquid nitrogen temperature (77 K). The measured transfer characteristics of Iricon 5-11-66 are shown for the standard and pulsed operations in Fig. 7. For this vidicon NEH decreases from 5.7×10^{-7} W/cm^2 at standard operation to 1.1×10^{-7} W/cm^2 for a $2V_{sl}(H)/V_{sl}(L)$ pulse ratio, which is a sensitivity improvement factor $(NEH)_{ss}/(NEH)_{op}$ of 5.2. Included on this figure are the transfer curves for pulse ratios of $V_{sl}(H)/V_{sl}(L)$ and $3V_{sl}(H)/V_{sl}(L)$, which have NEH's of 2.1×10^{-7} and 6.6×10^{-8} W/cm^2, respectively. Although the $3V_{sl}(H)/V_{sl}(L)$ pulse ratio provides a greater sensitivity improvement, overall Iricon performance is below that observed in the $2V_{sl}(H)/V_{sl}(L)$ mode because of increased image retention of target signals and sensing-layer blooming from spot imperfections. Dynamic response (DR) is increased by approximately 100%, while γ remains relatively constant at 0.80.

GE infrared vidicon Type Z7934 was used in these tests and has an extrinsic photoconductive sensing layer of copper-doped germanium that is counter-doped with antimony. The measured transfer characteristics of GE IR vidicon No. 326 for standard and pulsed operations is shown in Fig. 8. For the vidicon NEH decreased from 2.1×10^{-6} W/cm^2 at standard operation to 3.8×10^{-7} W/cm^2 at a $2V_{sl}(H)/V_{sl}(L)$ pulse ratio, which is a sensitivity improvement factor $(NEH)_{ss}/(NEH)_{op}$ of 6.8. At $3V_{sl}(H)/V_{sl}(L)$ the pulse ratio NEH is 3.1×10^{-7} W/cm^2, but the vidicon overall performance deteriorates because of sensing-layer nonuniformities. The dynamic range is increased by approximately 100% in all pulsed modes and remains relatively constant at 0.84.

The Westinghouse Thermicon used in these tests has a thermistor sensing layer of smoke-deposited arsenic trisulfide operable at ambient temperature (300 K). The measured transfer characteristics for Thermicon 6548054 for standard and pulsed operations is shown in Fig. 9. For this

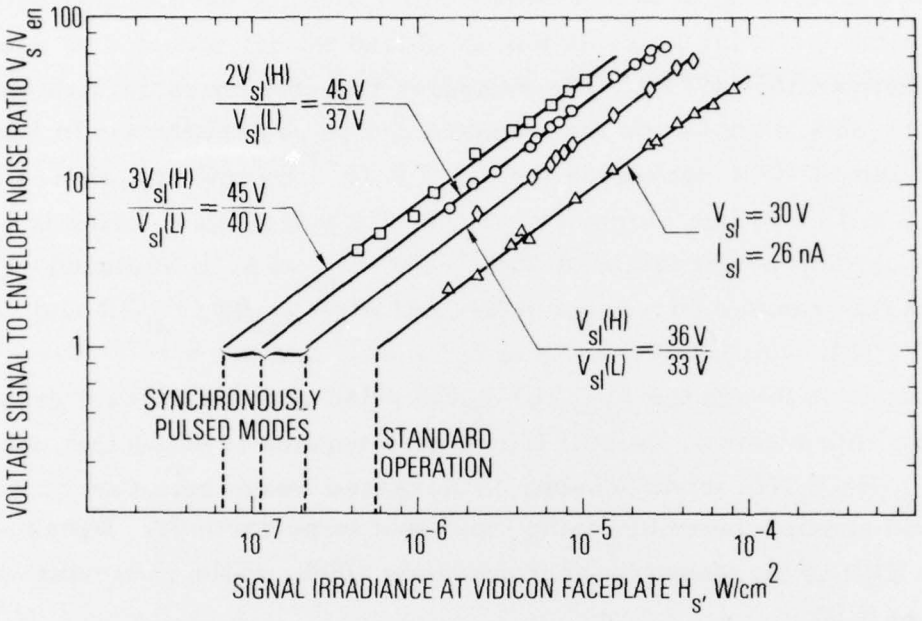

Fig. 7. Iricon Transfer Characteristics for Standard and Pulsed Operations. RCA Iricon 5-11-66. Spectral response 3.39 to 3.41 μm with filter at ambient.

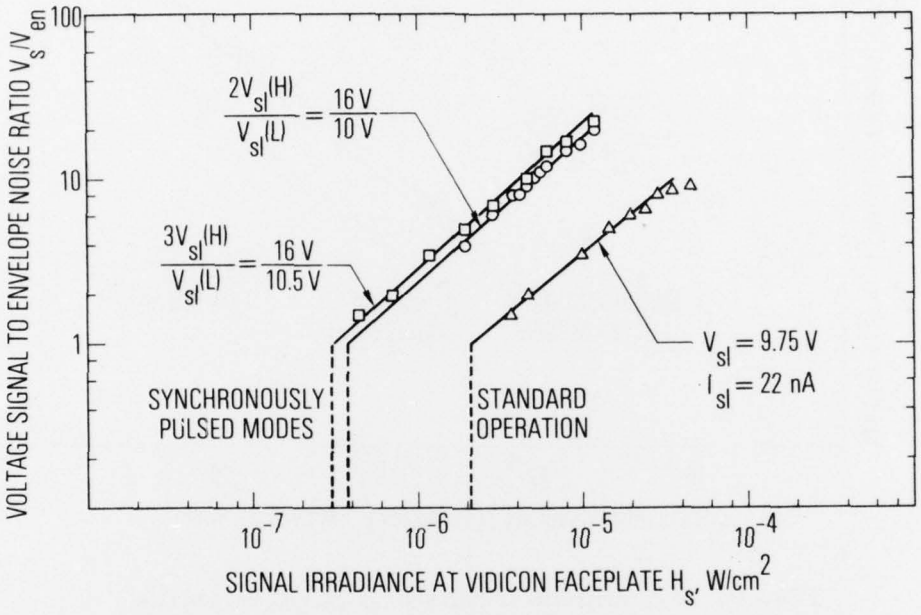

Fig. 8. GE Infrared Vidicon Transfer Characteristics for Standard and Pulsed Operations. GE Infrared Vidicon 326. Spectral response 3.39 to 3.41 μm with filter at ambient.

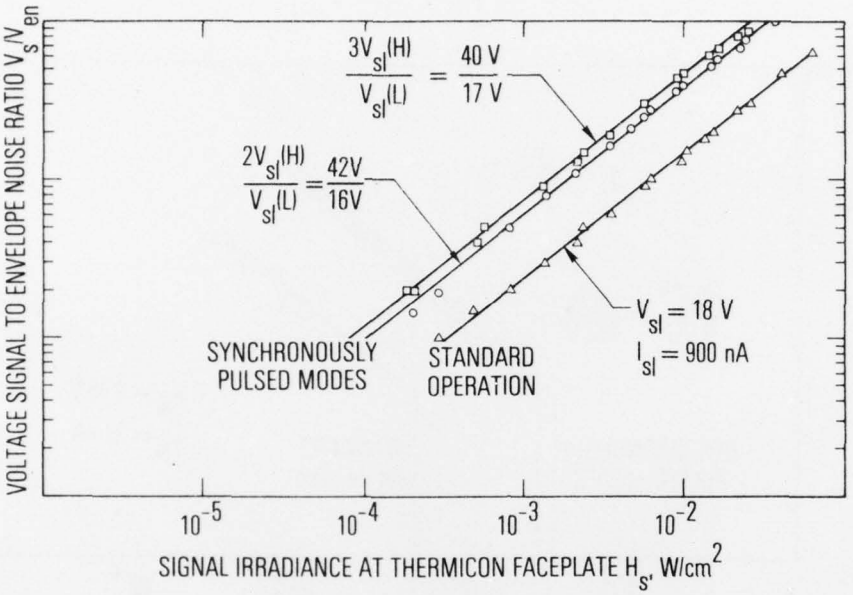

Fig. 9. Thermicon Transfer Characteristics for Standard and Pulsed Operations. Westinghouse Thermicon 6548056. Spectral response 8.11 to 13.89 μm with filter at ambient.

camera tube NEH decreases from 3.3×10^{-4} W/cm^2 at standard operation to 1.0×10^{-4} W/cm^2 at $2V_{sl}(H)/V_{sl}(L)$ pulse ratio. With a $3V_{sl}(H)/V_{sl}(L)$ pulse ratio NEH is 7.9×10^{-5} W/cm^2, but from the same reasons noted in the other vidicons tested overall performance is not at optimum. Dynamic response is increased by approximately 100% in all pulsed modes but r remains relatively constant at 0.78.

The RCA Type 7735A vidicon was used to evaluate this technique and has a photoconductive sensing layer of antimony trisulfide that is operable at ambient temperature. This conventional visible-light vidicon is used in commercial applications. The measured transfer characteristics of this camera tube for the standard and pulsed operations are shown in Fig. 10. On the bases of these data, NEH decreases from 2.45×10^{-7} W/cm^2 at standard operation to 8.1×10^{-8} W/cm^2 for a $2V_{sl}(H)/V_{sl}(L)$ pulse ratio. Included on this figure is the transfer curve for a $V_{sl}(H)/3V_{sl}(L)$ pulse ratio, which has a slightly higher NEH of 9.8×10^{-8} W/cm^2. The measured NEH at $3V_{sl}(H)/V_{sl}(L)$ pulse ratio was approximately equivalent to the value obtained with $2V_{sl}(H)/V_{sl}(L)$, but image retention was increased to an unacceptable level. Dynamic response in all pulsed-mode operations increases by approximately 50%, while γ remains relatively constant at 1.00.

The RCA Type 4532A vidicon was used to evaluate this technique and has a photoconductive sensing layer consisting of a two-dimensional array of silicon photodiodes operable at ambient temperature. Measured transfer characteristics for this camera tube in the standard and pulsed operations are shown in Fig. 11. From these data it is evident that NEH decreases from 9.7×10^{-9} W/cm^2 at standard operation to 2.2×10^{-9} W/cm^2 for a $V_{sl}(H)/3V_{sl}(L)$ pulse ratio. On the bases of these results, the sensitivity improvement factor for this vidicon is 4.4. When operated at a $V_{sl}(H)/V_{sl}(L)$ pulse ratio vidicon NEH was 7.2×10^{-10} W/cm^2. The same value for NEH was obtained when the vidicon was operated in the integrated saturation modes, i.e., $2V_{sl}(H)/V_{sl}(L)$ and $3V_{sl}(H)/V_{sl}(L)$. Dynamic response in the $V_{sl}(H)/3V_{sl}(L)$ pulse mode increases by approximately 50%, while γ remains constant at 0.73.

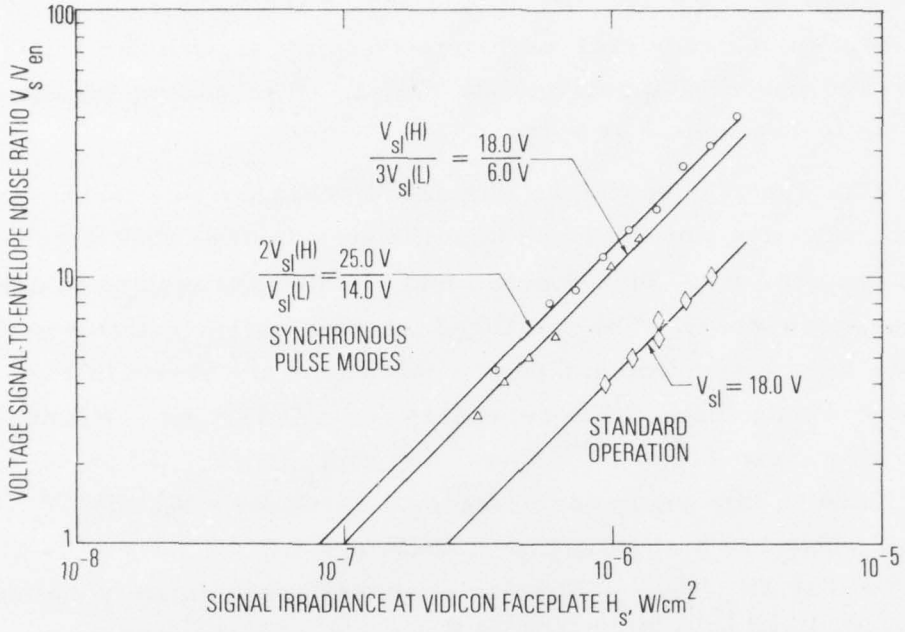

Fig. 10. RCA Visible-Light Vidicon Transfer Characteristics for Standard and Pulsed Operations. RCA Vidicon 7735A. Spectral response 0.616 to 0.637 μm with filter at ambient.

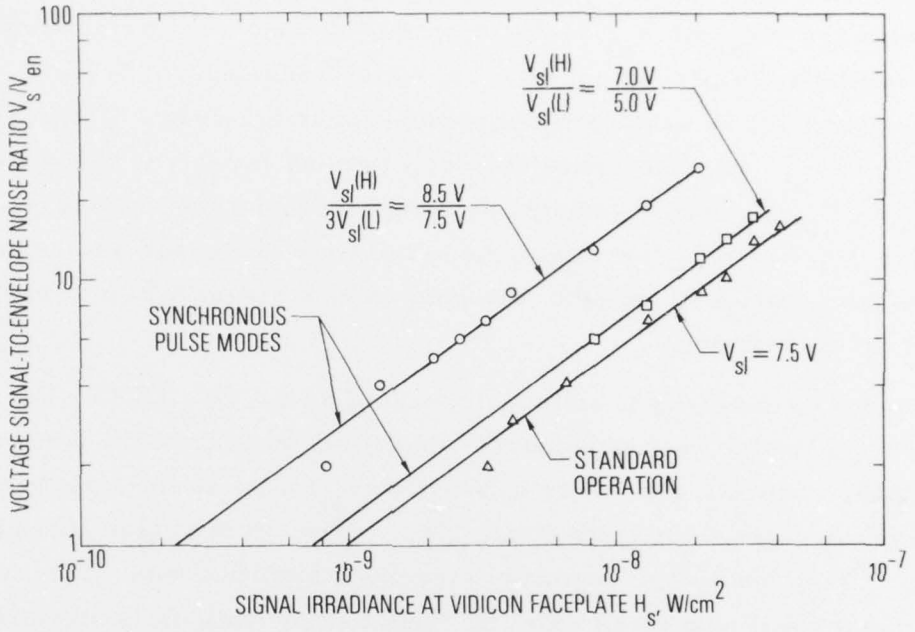

Fig. 11. RCA Silicon Diode Vidicon Transfer Characteristics for Standard and Pulsed Operations. RCA Vidicon 4532A. Spectral response 0.616 to 0.637 μm with filter at ambient.

A comparison of the improved camera-tube performance obtained with this novel pulsing technique is given in Table I. In all tests tube sensitivity NEH increased with the higher pulse ratio. For the infrared camera tubes tested the $2V_{sl}(H)/V_{sl}(L)$ ratio produced the best overall performance sensitivity improvement factors, which ranged from 3.3 to 5.5. This wide variation in sensitivity improvement is the result of differences in the dR_{sl}/dV_{sl} characteristics for each sensing layer. In these cases the $3V_{sl}(H)/V_{sl}(L)$ mode produced the greater improvement factors, which ranged from 4.2 to 8.6, but image-retention time increased and sensing-layer nonuniformities bloomed to the point where signal dynamic response was reduced significantly.

Standard visible-light vidicons operated at the $2V_{sl}(H)/V_{sl}(L)$ and $V_{sl}(H)/3V_{sl}(L)$ pulse ratios produced sensitivity improvement factors of 3.0 and 2.5, respectively. With a $3V_{sl}(H)/V_{sl}(L)$ ratio the improvement factor was approximately equivalent, i.e., ~ 3.0, to the value measured at $2V_{sl}(H)/V_{sl}(L)$, but image retention increased significantly. This lower improvement level measured with the visible-light vidicon is attributable to the voltage-resistance response and image-retention characteristics of the tube sensing layer. Compared to infrared camera tubes tested the Sb_2S_3 sensing layer has a smaller dR_{sl}/dV_{sl} slope and a longer image retention time.

The silicon diode vidicons operated at the $V_{sl}(H)/3V_{sl}(L)$ pulse ratio produced the optimum performance with sensitivity improvement factor of 4.4. This pulse mode is equivalent to blanking the beam readout for achieving signal integration. At a $3V_{sl}(H)/V_{sl}(L)$ pulse ratio the sensitivity improvement factor for the silicon diode vidicon was 1.3, which is equivalent to the value obtained for a $V_{sl}(H)/V_{sl}(L)$ pulse ratio. This very low improvement factor was anticipated because operating principles for the silicon diode sensing layer are different from those governing the other tubes. This vidicon derives the video signals from change accumulation

Table I. Camera-Tube-Performance Comparative Data

	RCA Iricon	Westinghouse Thermicon	General Electric IR Vidicon	RCA Visible-Light Vidicon	RCA Silicon-Diode Vidicon
NEH for Standard Operation, $(NEH)_{ss}$, W/cm^2	5.7×10^{-7}	3.3×10^{-4}	2.1×10^{-6}	2.45×10^{-7}	9.7×10^{-10}
V_{sl} Pulse Ratio for Optimum Performance $V_{sl}(H)/V_{sl}(L)$	$\frac{2V_{sl}(H)}{V_{sl}(L)}$	$\frac{2V_{sl}(H)}{V_{sl}(L)}$	$\frac{2V_{sl}(H)}{V_{sl}(L)}$	$\frac{2V_{sl}(H)}{V_{sl}(L)}$	$\frac{V_{sl}(H)}{3V_{sl}(L)}$
NEH at Optimum Pulse Ratio, $(NEH)_{op}$, W/cm^2	1.1×10^{-7}	1.0×10^{-4}	3.8×10^{-7}	8.1×10^{-8}	2.2×10^{-10}
Sensitivity Improvement Factor, $(NEH)_{ss}/(NEH)op$	5.2	3.3	5.5	3.0	4.4
NEH for $3V_{sl}(H)/V_{sl}(L)$ Pulse Rate, $(NEH)_{3V}$, W/cm^2	6.6×10^{-8}	7.9×10^{-5}	3.1×10^{-7}	8.1×10^{-8}	7.3×10^{-10}
Sensitivity Improvement Factor at $3V_{sl}(H)/V_{sl}(L)$, $(NEH)_{ss}/(NEH)_{3V}$	8.6	4.2	6.8	3.0	1.3

on the individual sensing-layer elements, which is in contrast to the more common mechanism of elemental changes in sensing-layer resistivity producing the video signals. Therefore since raising V_{sl} for more than one frame time has little effect on sensing-layer resistivity or capacitance the integrated-saturation mode does not increase tube sensitivity.

VI. CONCLUSIONS

This new electronic technique for synchronously pulsing the sensing-layer bias voltage can significantly enhance the detection capabilities of many types of image-forming sensors. When operated in the integrated-discharge mode, i.e., pulse ratios of $V_{sl}(H)/2V_{sl}(L)$ or more, the sensitivity of vidicon camera tubes increases and exceeds conventional operation by at least a factor of 3. For vidicons in which sensing-layer resistance varies widely with bias voltage greater increases in sensitivity are obtained when the integrated-saturation mode is used with $2V_{sl}(H)/V_{sl}(L)$ or $3V_{sl}(H)/V_{sl}(L)$ pulse ratio.

The infrared camera tubes operated in the integrated-saturation mode at $3V_{sl}(H)/V_{sl}(L)$ pulse ratios model exhibited increased image retention and blooming effects from spot imperfections although sensitivity improvement factors increased by approximately 25%. Visible-light vidicons operated at this same pulse ratio did not exhibit these detrimental image effects, but the sensitivity improvement factor was lower. Since these conventional image sensors have more uniform sensing layers with less spot imperfections it is anticipated that for the integrated-saturation mode higher pulse ratios, e.g., $4V_{sl}(H)/V_{sl}(L)$, and $5V_{sl}(H)/V_{sl}(L)$, can be used to effect greater sensitivity from such vidicons without any loss in overall image quality.

Significant increases in sensitivity can be attained from silicon-diode vidicons operated in the integrated-discharge mode. Only slight improvement is achieved with this type of vidicon when operated in the integrated-saturation mode. Since performance of silicon-diode vidicons is not a function of resistive changes but determined by charge accumulation on each sensing-layer element, the observed sensitivity difference between these two pulse modes is consistent with physical models.

From data contained in this paper it is predicted that the synchronous-pulse technique can improve sensitivity not only of most types of vidicon image sensors but also some solid-state image sensors. The technique is applicable to solid-state imaging devices in which (1) the sensing-layer elements have signal integration properties similar to those in vidicons and, (2) the electronic video output is derived from a readout mechanism that sequentially interrogates each sensing element. The specific solid-state image-forming sensors that would most likely exhibit signal enhancement when these pulse techniques are the charge injection device (CID) image sensor and the Schottky barrier diode arrays.

LABORATORY OPERATIONS

The Laboratory Operations of The Aerospace Corporation is conducting experimental and theoretical investigations necessary for the evaluation and application of scientific advances to new military concepts and systems. Versatility and flexibility have been developed to a high degree by the laboratory personnel in dealing with the many problems encountered in the nation's rapidly developing space and missile systems. Expertise in the latest scientific developments is vital to the accomplishment of tasks related to these problems. The laboratories that contribute to this research are:

Aerophysics Laboratory: Launch and reentry aerodynamics, heat transfer, reentry physics, chemical kinetics, structural mechanics, flight dynamics, atmospheric pollution, and high-power gas lasers.

Chemistry and Physics Laboratory: Atmospheric reactions and atmospheric optics, chemical reactions in polluted atmospheres, chemical reactions of excited species in rocket plumes, chemical thermodynamics, plasma and laser-induced reactions, laser chemistry, propulsion chemistry, space vacuum and radiation effects on materials, lubrication and surface phenomena, photosensitive materials and sensors, high precision laser ranging, and the application of physics and chemistry to problems of law enforcement and biomedicine.

Electronics Research Laboratory: Electromagnetic theory, devices, and propagation phenomena, including plasma electromagnetics; quantum electronics, lasers, and electro-optics; communication sciences, applied electronics, semiconducting, superconducting, and crystal device physics, optical and acoustical imaging; atmospheric pollution; millimeter wave and far-infrared technology.

Materials Sciences Laboratory: Development of new materials; metal matrix composites and new forms of carbon; test and evaluation of graphite and ceramics in reentry; spacecraft materials and electronic components in nuclear weapons environment; application of fracture mechanics to stress corrosion and fatigue-induced fractures in structural metals.

Space Sciences Laboratory: Atmospheric and ionospheric physics, radiation from the atmosphere, density and composition of the atmosphere, aurorae and airglow; magnetospheric physics, cosmic rays, generation and propagation of plasma waves in the magnetosphere; solar physics, studies of solar magnetic fields; space astronomy, x-ray astronomy; the effects of nuclear explosions, magnetic storms, and solar activity on the earth's atmosphere, ionosphere, and magnetosphere; the effects of optical, electromagnetic, and particulate radiations in space on space systems.

THE AEROSPACE CORPORATION
El Segundo, California